Journal of Hydrology (2007) 332, 487–496

available at www.sciencedirect.com

journal homepage: www.elsevier.com/locate/jhydrol

Resampling of regional climate model output for the simulation of extreme river flows

Robert Leander *, T. Adri Buishand

Royal Netherlands Meteorological Institute (KNMI), P.O. Box 201, 3730 AE De Bilt, The Netherlands

Received 14 February 2006; received in revised form 7 August 2006; accepted 8 August 2006

KEYWORDS
Meuse basin;
Regional climate models;
Stochastic precipitation modelling;
Hydrological modelling;
Extreme values

Summary The objective of this paper is to investigate whether resampling of the output from a regional climate model (RCM) can provide realistic long-duration sequences of precipitation and temperature for the simulation of extreme river flows. This is important to assess the impact of climate change on river flooding. Daily streamflows of the river Meuse in western Europe are considered. Resampling is performed with a nearest-neighbour technique that was already successfully applied to the observed daily precipitation and temperature in the river basin. Streamflows are simulated with the semi-distributed HBV rainfall–runoff model. Two simulations of the KNMI regional climate model RACMO are considered. One of these simulations is driven by the global atmospheric model HadAM3H of the UK Meteorological Office for the period 1961–1990 and the other by ERA40 re-analysis data. Much attention is given to the bias correction of RACMO precipitation. It was found that a relatively simple nonlinear correction adjusting both the biases in the mean and variability led to a better reproduction of observed extreme daily and multi-day precipitation amounts than the commonly used linear scaling correction. This also resulted in more realistic discharge extremes, suggesting that a correct representation of the variability of precipitation is important for the simulation of extreme flood quantiles. For the Meuse basin it is further shown that it is advantageous to correct for the variability of the 10-day precipitation amounts rather than that of the daily amounts. Despite the remaining biases in the RCM data, the simulated extreme flood quantiles correspond quite well with those obtained using observed precipitation and temperature.

Introduction

General Circulation Models (GCMs) are considered to be the most advanced tools currently available for simulating the response of the global climate system to changing atmospheric composition (Mearns et al., 2001). There is a great interest in the impact of the climate changes projected by these models on river flooding (e.g., Prudhomme et al.,

* Corresponding author. Tel.: +31 30 2206429; fax: +31 30 2210407.
E-mail address: leander@knmi.nl (R. Leander).

0022-1694/$ - see front matter © 2006 Elsevier B.V. All rights reserved.
doi:10.1016/j.jhydrol.2006.08.006

2002). It is well known that the magnitude of the climate change impact depends partly on the characteristics of the river basin (e.g., Arnell and Reynard, 1996; Nijssen et al., 2001). Hydrological simulations are therefore needed to assess this impact. However, the precipitation produced by GCMs is generally not suitable to feed into hydrological models, partly because of the coarse spatial resolution of GCMs. A downscaling procedure is therefore needed to provide the required input. One approach is to use a high resolution Regional Climate Model (RCM), driven by lateral boundary conditions from the GCM of interest. The popularity of this approach is growing, due to increased computer resources and the enhanced performance of RCMs and processing. Recent applications are presented by Kay et al. (2006), who used a high resolution RCM to assess changes in flood frequency for 15 catchments in the UK, and Lenderink et al. (in press), who investigated future discharges of the river Rhine.

A problem with the use of RCMs for hydrological purposes is that the simulated precipitation differs systematically from the observed precipitation (e.g., Frei et al., 2003). Lenderink et al. (in press) corrected for this bias by applying a (seasonally and spatially varying) correction factor, while Hay et al. (2002) made use of the gamma distribution to match the distribution of the modelled daily precipitation with that of observed daily precipitation. Arnell et al. (2003), on the other hand, did not use any bias correction.

Apart from the bias in the simulated precipitation, the estimation of flood quantiles suffers from the limited length of the RCM simulations (usually no longer than 30 years for present-day models). A strong extrapolation of the distribution of the simulated discharges is then needed to estimate the extreme flood quantiles if the hydrological model is run directly with the (bias-corrected) RCM output.

In this paper both problems are tackled for the basin of the river Meuse upstream of Borgharen in the Netherlands (drainage area approximately 21,000 km^2). This part of the basin is located in eastern Belgium and northeastern France. In an earlier study, long-duration sequences of daily precipitation and temperature have been generated for the considered basin by resampling from observed data using a nearest-neighbour technique (Leander et al. (2005), from here on LBAW05). Here, this weather generator is applied to RCM output instead of observed data. After bias correction the resampled data are used for streamflow simulations using a semi-distributed hydrological model. The objective of this study is to establish whether the use of RCM output in a hydrological model can yield extreme discharges (up to return periods in the order of 1000 years). Simulated extreme discharges from bias-corrected RCM output are compared with those based on observed meteorological data.

This paper is organized as follows: First the use of RCM output and the applied bias corrections are discussed. Then the resampling algorithm is briefly explained. The autocorrelation of daily precipitation and the distribution of 10-day winter maxima of basin-average precipitation from long-duration resampled sequences are compared with those from observed precipitation. Subsequently, the hydrological simulations are described and results of extreme discharges are shown. The paper closes with a summary and a short discussion on the usefulness of the presented approach.

RCM output for the Meuse basin

The KNMI model RACMO

In this study the output of the KNMI regional climate model RACMO (Regional Atmospheric Climate MOdel) was used (Lenderink et al., 2003). This model has a resolution of about 50 km. Its domain roughly stretches from 40 °W to 50 °E and from 30 °N to 70 °N. The Meuse basin is located in the center of the domain and is almost covered by 15 grid boxes, as shown in Fig. 1. For the hydrological simulations the Meuse basin is subdivided into 15 subbasins. The modelled area-average precipitation for each of the subbasins was obtained as a weighted average over the grid boxes covering the subbasin. The weights were determined as the fraction of the subbasin area falling within a specific grid box, using a 2.5 km × 2.5 km grid. The nearest grid box was assigned to those parts of the basin that were not covered by the 15 grid boxes.

Two multi-year RACMO runs were made available. In the framework of the EU-funded project PRUDENCE (Prediction of Regional scenarios and Uncertainties for Defining EuropeaN Climate change risks and Effects, see, e.g., Christen-

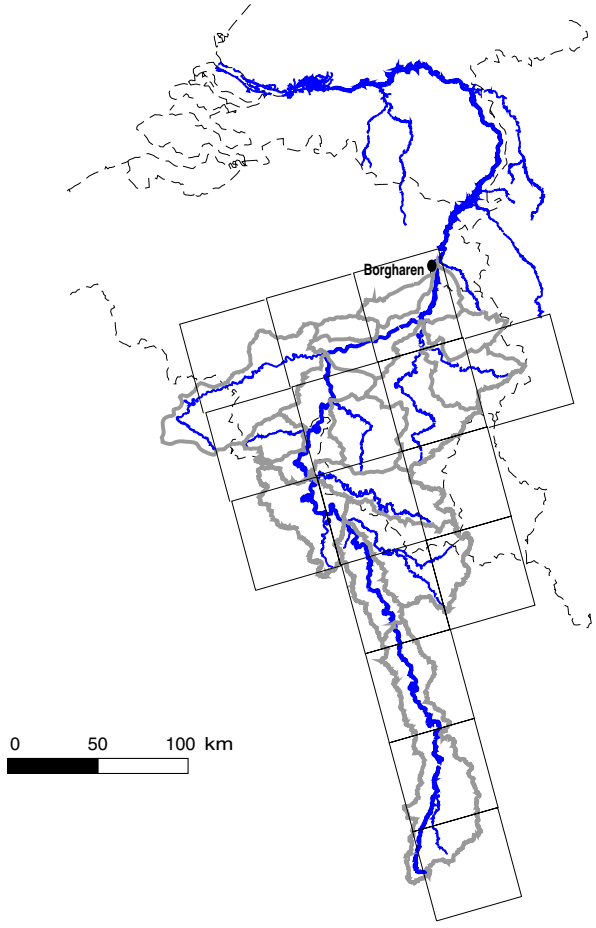

Figure 1 Locations of the 15 RACMO grid boxes used in this study, relative to the Meuse subbasins (thick grey contours) and the river Meuse with tributaries. State boundaries (dashed) and the location of the gauging station Borgharen are also shown.

sen and Christensen (in press), RACMO was driven by lateral boundaries from the atmospheric model HadAM3H (short for Hadley Centre Atmospheric Model 3, High resolution) of the Hadley Centre of the UK Meteorological Office. HadAM3H works at a resolution of 1.25° in latitude and 1.875° in longitude, corresponding to a resolution of about 150 km near the RACMO domain. It uses the observed sea-surface temperature and sea ice for the reference period 1961–1990 (Jones et al., 2001). The second RACMO run was driven by 40 years of re-analysis data (ERA40) of the European Centre for Medium-Range Weather Forecasting (Uppala et al., 2005). A re-analysis is an estimate of the state of the atmosphere, based on observations and a numerical weather forecast. Its circulation is therefore expected to be more realistic than that of any GCM. Hence, the comparison between a GCM-driven RCM run and one driven by re-analysis data provides insight into the influence of the driving GCM on the considered RCM run. The forecast model used for the re-analysis is operated at a resolution of about 125 km. RACMO uses data from either the driving GCM (HadAM3H) or the re-analysis to set the boundary conditions of the horizontal velocity, heat and moisture (on all vertical levels) and the sea-level pressure. Details on the RACMO model can be found in Lenderink et al. (2003).

From the ERA40-driven RACMO run the data were extracted for the 30-year period 1969–1998 in order to have two runs of the same length. The period 1969–1998 was preferred to 1961–1990, because streamflow simulations with observed data were available for that period (LBAW05). With the simulation driven by ERA40 boundaries it is possible to discriminate between the bias resulting from the driving HadAM3H GCM and the bias introduced by RACMO.

For each of the subbasins the interpolated area-average precipitation was compared with the corresponding subbasin precipitation for the historical reference period 1969–1998. For the Belgian subbasins, these averages were calculated from daily station values (using Thiessen interpolation) by the Royal Meteorological Institute of Belgium (RMIB). For the French subbasins, the areal precipitation was obtained from the data of 63 stations using squared inverse distance interpolation on a regular grid. The left panel of Fig. 2 shows an area-weighted average of the relative bias of the mean daily precipitation amount in each calendar month. The largest biases are found in the winter half-year (October–March), on average 26% in the HadAM3H-driven run and 16% in the ERA40-driven run. Except for a few months, the HadAM3H-driven run shows a larger bias than the ERA40-driven run. The relative bias of the HadAM3H-driven run is comparable with that found for the regional climate models HadRM2 (Shabalova et al., 2003) and HadRM3H (Lenderink et al., in press) of the Hadley Centre for the adjacent Rhine basin. The wet bias is partly a result of the fact that the observed precipitation amounts were not corrected for the systematic undercatch inherent to rain gauges. Frei et al. (2003) report a systematic undercatch of about 8% for the lowland stations in the Alps (below 600 m). For the Meuse basin (almost entirely below 600 m), the undercatch may differ somewhat from this value, due to climatological differences and other types of rain gauges. It is unlikely that all precipitation biases found here are due to undercatch.

The right panel of Fig. 2 presents the basin-average temperature bias. This bias refers to the difference between the area-weighted average T_{area} of the subbasin temperatures obtained from RACMO and the Thiessen average $T_{stations}$ of 11 stations, serving as a reference temperature. The bias in the HadAM3H-driven run is similar to that in the ERA40-driven run, except for October, which is colder and the period December–February, which is warmer than in the ERA40-driven run.

van Ulden et al. (in press) analyzed the circulation bias of HadAM3H for Europe. They report a positive bias in the strength of the westerlies in winter, leading to a wetter and milder climate. This is consistent with the relatively large positive bias in precipitation and temperature in the HadAM3H-driven run during winter.

Table 1 compares several characteristics of daily precipitation from both RACMO runs with those of the observed precipitation. Results are presented for the winter half-year as well as the summer half-year (April–September). The coefficient of variation (CV) displayed in this table is defined as the ratio between the sample standard deviation and the sample mean. Both RACMO runs show a considerable underestimation of the CV of the daily precipitation amounts in the winter half-year. The overestimation of the mean daily precipitation in winter is accompanied by an overestimation of the fraction of wet days in both the HadAM3H-driven and

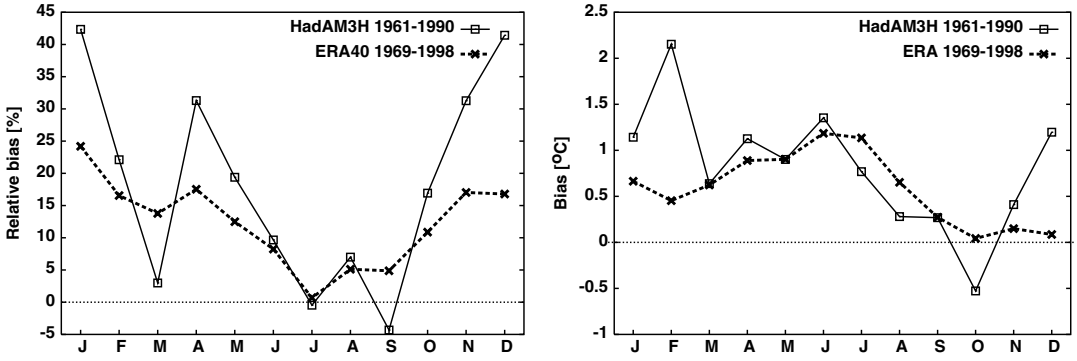

Figure 2 Basin-average relative bias in the monthly precipitation (left) and absolute bias in the mean monthly temperature (right). The HadAM3H-driven run for the period 1961–1990 and the ERA40-driven run for the period 1969–1998 are compared with the observations for the period 1969–1998.

Table 1 Mean, coefficient of variation (CV) and lag 1 autocorrelation coefficient r_1 of daily precipitation, fraction f_{wet} of wet days (with 0.3 mm or more), mean wet-day amount m_{wet} and correlation r_s between the daily precipitation amounts in different subbasins for the observations and both RACMO runs

	Winter half-year			Summer half-year		
	Observed	HadAM3H	ERA40	Observed	HadAM3H	ERA40
Mean (mm/day)	2.78	3.49	3.20	2.40	2.64	2.59
CV	1.73	1.48	1.46	1.81	1.69	1.79
r_1	0.37	0.35	0.34	0.27	0.25	0.24
f_{wet} (%)	55.79	67.91	68.34	50.28	57.13	56.13
m_{wet} (mm/day)	4.94	5.10	4.65	4.75	4.58	4.57
r_s	0.85	0.90	0.90	0.73	0.81	0.82

With the exception of r_s, all statistics are area-weighted averages over subbasins. The statistic r_s is averaged over all pairs of subbasins. Results are given for the winter half-year (October–March) as well as the summer half-year (April–September).

ERA40-driven run, whereas the mean wet-day amount is rather well preserved. There are also too many wet days in the summer half-year in both RACMO simulations. In the HadAM3H-driven run the lag 1 autocorrelation coefficient r_1 of daily precipitation is slightly underestimated in both seasons. The bias in r_1 is even somewhat larger in the ERA40-driven run. This bias is mainly due to the inability of RACMO to reproduce the relatively large values of r_1 for the French part of the basin ($r_1 = 0.40$ in the winter half-year, compared to $r_1 = 0.35$ for the Belgian part in the winter half-year). The correlation r_s between the precipitation amounts in different subbasins is higher than observed in both runs, in the summer as well as the winter half-year. The differences between the HadAM3H-driven and ERA40-driven runs are small, suggesting that the bias is mainly an artefact of RACMO.

Bias correction

Because the bias in precipitation and temperature was found to vary spatially, bias corrections were carried out for each subbasin individually. For precipitation a simple linear correction using a scaling factor was compared with a slightly more advanced nonlinear correction. To reduce the effect of sampling variability, the scaling factor was determined for every five-day period of the year as the ratio between the average observed precipitation and that of the RACMO run in a window including the 30 days before and after the considered five-day period.

The linear correction adjusts the mean precipitation, but leaves the CV unaffected, because both mean and standard deviation are multiplied by the same factor. As an alternative, a power transformation was studied, which corrects the CV as well as the mean. In this nonlinear correction each daily precipitation amount P is transformed to a corrected amount P^* using

$$P^* = aP^b \tag{1}$$

Shabalova et al. (2003) used this expression to modify observed 10-day precipitation amounts in order to obtain a scenario of a future climate with a changed mean and CV. For the estimation of the parameters a and b they assumed that these 10-day precipitation amounts have a Weibull distribution. For the daily precipitation amounts in the Meuse basin this assumption is too restrictive. The parameters a and b were therefore obtained with a distribution-free approach. As in the case of the linear scaling factor, these parameters were estimated for each five-day period, using the same 65-day window. First, the value of b was determined such that the CV of the corrected daily precipitation matched that of the observed daily precipitation. This was done iteratively, using a root-finding algorithm. The factor a was then determined such that the mean of the transformed daily values corresponded with the observed mean. The resulting value of a depends on b. By contrast b depends only on the CV and its determination is independent of the value of a. The left panel of Fig. 3 displays the annual cycle of the exponent b for both RACMO runs.

A value greater than unity indicates that the CV of the precipitation is enhanced by the correction. In the HadAM3H-driven run this is the case throughout the year. In the ERA40-driven run the correction reduces the CV in the months June, July and August. The correspondence between the two curves suggests that the bias in the CV originates from RACMO itself rather than the driving GCM.

As an alternative a and b can be chosen such that two different quantiles Q_{p1} and Q_{p2} of the corrected precipitation match those of the observations. Since the transformation in Eq. (1) is monotone, the quantiles of the transformed daily precipitation amounts are simply obtained by applying the same transformation to the quantiles of the uncorrected daily precipitation amounts from RACMO $Q_{p1,R}$ and $Q_{p2,R}$. From the requirement that

$$aQ_{p1,R}^b = Q_{p1,O} \quad \text{and} \quad aQ_{p2,R}^b = Q_{p2,O} \tag{2}$$

where $Q_{p1,O}$ and $Q_{p2,O}$ are the corresponding observed quantiles, it follows by elimination of a and taking logarithms that

$$b = \frac{\log(Q_{p2,O}/Q_{p1,O})}{\log(Q_{p2,R}/Q_{p1,R})} \tag{3}$$

For the HadAM3H-driven run the values of b obtained from Eq. (3) with p1 = 65, p2 = 99 and p1 = 65, p2 = 95 were compared with those fitted on the CV. The 65% quantile roughly corresponds with the mean daily precipitation amount. The results are shown in the right panel of Fig. 3. The curve based on Q_{65} and Q_{99} closely follows that based on the CV, except for small deviations in summer. Taking Q_{95}, instead of Q_{99}, results in slightly larger values of b. In order to cope with bias in the variability of multi-day amounts, the use of

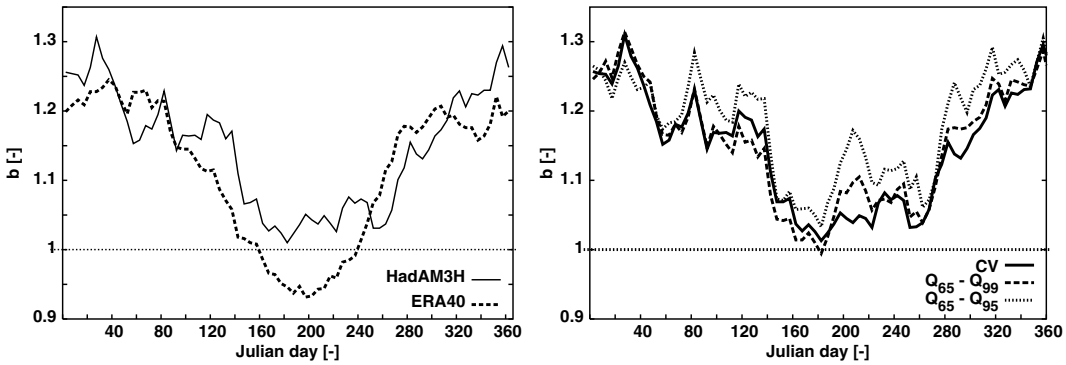

Figure 3 Annual cycle of the area-averaged exponent b in Eq. (1). On the left the exponents derived for the HadAM3H-driven run and the ERA40-driven run are shown. On the right the values of b based on the CV and those based on two different pairs of quantiles: Q_{65}—Q_{99} and Q_{65}—Q_{95} are given for the HadAM3H-driven run.

the CV is preferred to determine the parameter b in Eq. (1) of this paper.

Fig. 4 shows the basin-averaged exponential probability plots of daily precipitation for the winter half-year for both RACMO runs. The plots clearly illustrate the effect of both corrections. After applying the linear bias correction to the RACMO precipitation, the intermediate quantiles (exceedance probabilities > 0.1) agree better with the observed quantiles, but the more extreme quantiles (exceedance probabilities < 0.1) are too low and actually worse than those for the uncorrected data. This is consistent with the underestimation of the CV. With the nonlinear correction it is possible to adjust both the intermediate and the more extreme quantiles of the distribution, while keeping the number of parameters in the correction formula at a minimum. For the summer half-year, the effect of the nonlinear correction is smaller (not shown), because the bias in the CV is smaller in this season, as shown in Table 1.

Though the distribution of the nonlinearly corrected daily precipitation amounts resembles that of the observations quite satisfactorily, this is not necessarily true for the distribution of the multi-day precipitation amounts. Large multi-day events can be more important for the generation of floods than an extreme daily event. Extreme flows in the lower part of the Meuse basin are often associated with large multi-day precipitation totals in winter over periods of about 10 days, rather than extreme daily events (Tu, 2006). Fig. 5 is similar to Fig. 4, but now for the (non-overlapping) 10-day precipitation amounts. For the HadAM3H-driven run the nonlinear correction leads to a better agreement with the observations than the linear correction. The same is found for the ERA40-driven run, but the larger quantiles of the distribution of the 10-day precipitation amounts (exceedance probabilities < 0.1) are still somewhat underestimated. This is partly due to an additional negative bias in the autocorrelation of the daily values, resulting from the nonlinear transformation of the data. The autocorrelation generally decreases if a value of $b > 1$ is needed to increase the CV, as is demonstrated in ''Resampling of RCM output''. This decrease of the autocorrelation leads to a decrease of the standard deviation of the multi-day precipitation amounts, resulting in an underestimation of the large quantiles of these amounts. The most obvious and least complicated solution to this problem is to 'overcompensate', i.e., to use a larger value of b, such that the CV of the n-day totals, CV_n, of the transformed RACMO precipitation equals that of the n-day totals of the observations for some $n > 1$.

In Fig. 6 the observed values of CV_n for $n \leqslant 15$ are compared to those of uncorrected and corrected RACMO data for two different nonlinear corrections, one based on CV_1 and one based on CV_{10}. For the uncorrected RACMO data

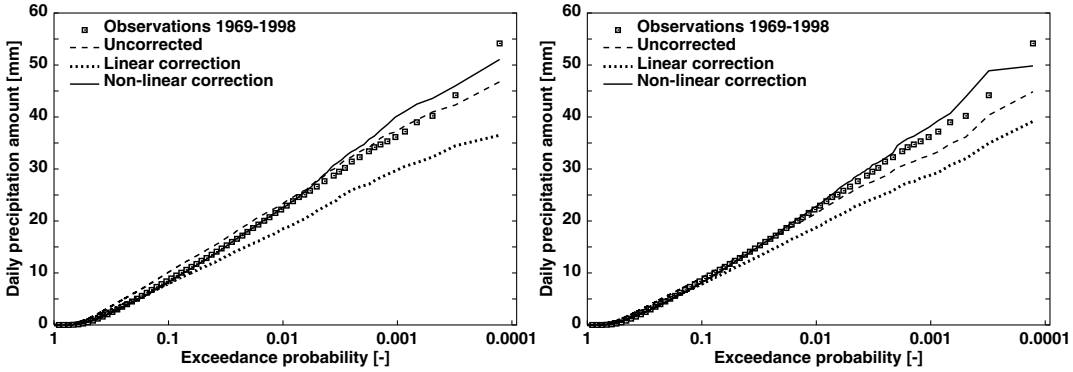

Figure 4 Exponential probability plots of the daily precipitation in the winter half-year, averaged over individual subbasins for the HadAM3H-driven run (left) and the ERA40-driven run (right). The plots for the uncorrected, linearly corrected and nonlinearly corrected precipitation are compared to the plot for the observed precipitation.

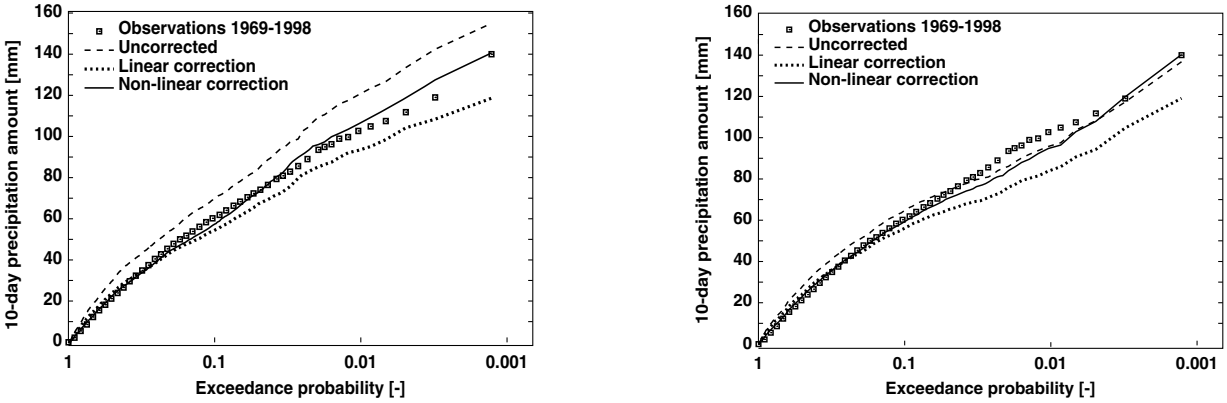

Figure 5 Similar to Fig. 4, but now for the 10-day precipitation amounts (left HadAM3H, right ERA40).

all CV_n are underestimated. With a nonlinear correction based on CV_1, the multi-day CVs improve, but they are still too low, in particular for the ERA40-driven run. With a nonlinear correction based on CV_{10} the underestimation of the multi-day CVs disappears, at the cost of an overestimation of CV_1 and CV_2.

Fig. 7 shows how the exponential probability plot of the 10-day precipitation amounts of the ERA40-driven run changes due to fitting b on CV_{10} instead of CV_1. The correction based on CV_{10} results in a better correspondence with the observed 10-day precipitation amounts, due to a slightly larger value of b in the correction.

The bias correction of temperature is more straightforward than that of precipitation, involving shifting and scaling to adjust the mean and variance, respectively. For each subbasin, the corrected daily temperature T^* was obtained as

$$T^* = \overline{T} + \frac{\sigma(T_{\text{stations}})}{\sigma(T_{\text{area}})}(T - \overline{T}) + (\overline{T}_{\text{stations}} - \overline{T}_{\text{area}}) \quad (4)$$

where T is the uncorrected daily temperature from RACMO, T_{stations} is the Thiessen average for the basin of observed temperatures from 11 stations, and T_{area} is the corresponding basin-average temperature obtained from RACMO. In this equation an overbar denotes the 30-year average and σ the standard deviation. Both statistics were determined for each 5-day period of the year separately, using the same 65-day window as for the bias correction of daily precipitation. A similar transformation was used by Shabalova et al. (2003) to perturb observed temperature with the changes of the mean and standard deviation projected by an RCM scenario run. Note that the temperature anomalies were scaled by the same factor for all subbasins and the temperature means were shifted by the same offset. The annual cycle of the scaling factor is shown in Fig. 8. The deviation from

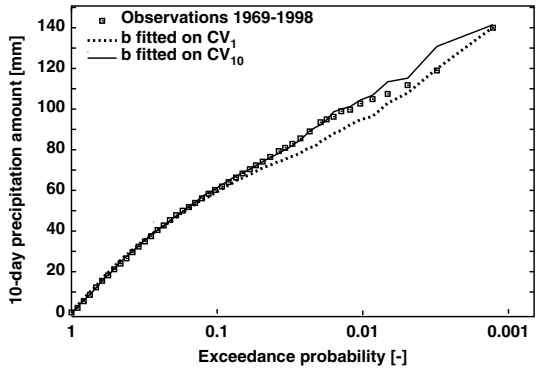

Figure 7 Exponential probability plots of the 10-day precipitation amounts in the winter half-year for the ERA40-driven run, after a nonlinear correction of the daily precipitation amounts with b fitted on CV_1 and CV_{10}, respectively.

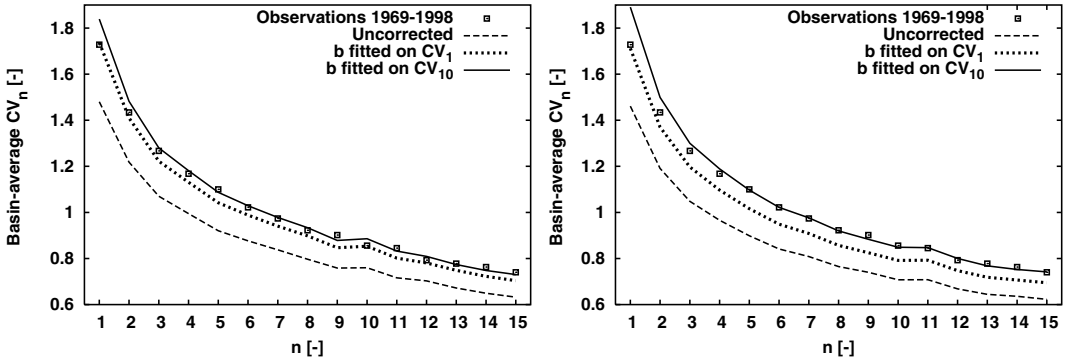

Figure 6 Basin-average coefficient of variation of n-day precipitation amounts CV_n for the HadAM3H-driven run (left) and the ERA40-driven run (right) for the winter half-year. The uncorrected runs and the nonlinearly corrected runs based on CV_1 and CV_{10} are compared with the observations.

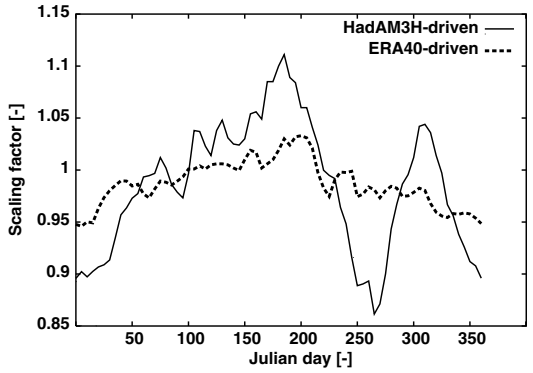

Figure 8 Annual cycle of the scaling factors applied to correct the standard deviation of the daily temperature from the HadAM3H-driven run and the ERA40-driven run, respectively.

unity is within 0.15 for the HadAM3H-driven run and nearly always less than 0.05 for the ERA40-driven run. Roughly the same factors were obtained for individual grid boxes containing one or more temperature stations.

Resampling of RCM output

Nearest-neighbour resampling is a simulation method which requires no assumptions concerning the underlying probability distributions or dependencies between variables (Rajagopalan and Lall, 1999; Buishand and Brandsma, 2001). In this study the algorithm described by LBAW05 was used to generate 3000-year sequences of daily precipitation and temperature for the 15 subbasins of the Meuse by sampling with replacement from the 30-year RACMO runs. In this algorithm, sampling of new days is conditioned on the area-weighted average of standardized subbasin precipitation and temperature of the previous day, and the average of standardized precipitation of a number of preceding days, which act as a memory for the simulation. A moving window is used to restrict the search for nearest neighbours to the season of interest.

In LBAW05, resampling was based on station data. Here resampling was driven by the uncorrected RACMO subbasin data. Furthermore, a five-day memory and a moving window of 121 days were used, instead of a four-day memory and a 61-day moving window in order to improve the simulation of extreme multi-day precipitation amounts. The bias corrections described earlier were applied afterwards to the resampled 3000-year sequences.

It was shown in LBAW05 that the resampling algorithm described above preserves the autocorrelation of its base material quite well. However, it was seen in Table 1 that RACMO tends to underestimate the lag 1 autocorrelation of daily precipitation and a nonlinear bias correction influences the autocorrelation. Fig. 9 compares the basin-average autocorrelation coefficients of corrected and uncorrected resampled precipitation for both RACMO runs with those observed for the winter half-year. For the observations also the standard errors *se* were calculated, using the jackknife method of Buishand and Beersma (1993). Apart from a significant negative bias in the lag 1 autocorrelation, the uncorrected resampled data from the HadAM3H-driven run reproduce the autocorrelation coefficients quite well. The transformation in Eq. (1), however, results in a decrease of the autocorrelation coefficients, in particular for shorter time lags in the winter half-year. The resampled data from the ERA40-driven run show a larger bias in the autocorrelation coefficients than those from the HadAM3H-driven run. Transformation based on CV_{10} leads to a further decrease of the autocorrelation coefficients. The effect of this decrease on the variability of the 10-day precipitation amounts is compensated by an overestimation of CV_1. The nonlinear correction also leads to a slight decrease of the spatial correlation r_s of the daily precipitation amounts (not shown). The spatial correlation of the nonlinearly corrected sequences remains, however, too high. This bias has little effect on the simulated floods for the Meuse, because these are more sensitive to the spatial correlation of the 10-day precipitation amounts. The latter is better reproduced by RACMO than r_s.

In Fig. 10 the 10-day winter maxima of basin-average precipitation from observations and those from the resampled 3000-year sequences for both RACMO runs are shown. Each plot displays the average ordered maxima of three independent sequences of 3000 years. The plot for the

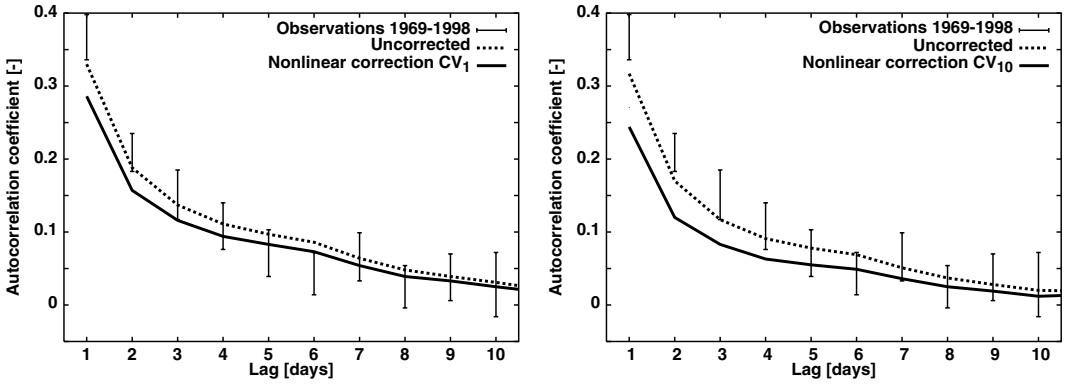

Figure 9 The basin-average autocorrelation coefficients of the observed daily precipitation, the 3000-year resampled HadAM3H-driven run (left) and the ERA40-driven run (right) for the winter half-year, before and after the nonlinear correction. The autocorrelation coefficients of the observations are represented by error bars, which indicate the $2 \times se$-intervals of the coefficients.

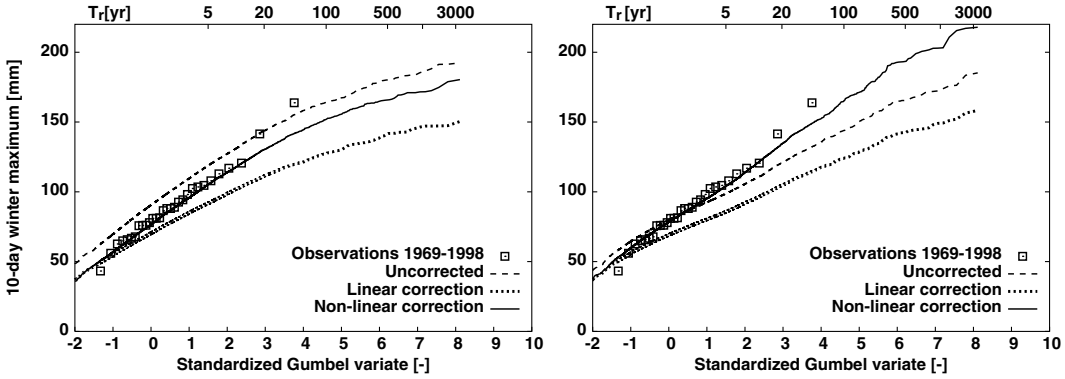

Figure 10 Winter maxima of basin-average 10-day precipitation amounts from resampled RCM data (9000 years), either uncorrected or after applying a linear correction or a nonlinear correction, compared with observed precipitation. The exponent b of the nonlinear correction was based on CV_1 for the HadAM3H-driven run in the left panel and on CV_{10} for the ERA40-driven run in the right panel. The upper horizontal axes indicate the mean recurrence time T_r (return period) in years.

nonlinearly corrected data corresponds quite well with that of the observations. A linear correction appears to be worse than no correction at all.

Hydrological simulations

In this study the semi-distributed HBV model, developed at the Swedish Meteorological and Hydrological Institute, was used for rainfall–runoff modelling (Lindström et al., 1997). This model describes hydrological processes on subbasin scales, such as soil moisture storage and fast and slow runoff, in terms of water balances of reservoirs. A simplified Muskingum algorithm was used to simulate flood routing along the river (Booij, 2005). The schematization and parameters were the same as in LBAW05. Basin-average temperatures of the subbasins were used instead of station data. Daily values of potential evapotranspiration (PET) for the Belgian subbasins were made available by RMIB. Since similar PET values for the French subbasins were not available, the average over the Belgian part of the basin was used for these subbasins. In the hydrological simulations with RACMO output, PET was derived for each of the subbasins from the daily temperature T using the relation:

$$\mathrm{PET} = [1 + \alpha_m(T - \overline{T}_m)]\overline{\mathrm{PET}}_m \quad (5)$$

with $\overline{T}_m$ the mean observed temperature (°C) and $\overline{\mathrm{PET}}_m$ the mean observed PET (mm day^{-1}) for calendar month m in the period 1967–1998. $\overline{T}_m$ was obtained from the average of the four nearest stations to the subbasin of interest using an altitude correction of −0.6 °C/100 m. In the simulation with bias-corrected (resampled) RACMO output, the bias-corrected (resampled) temperature T^* was used for T in Eq. (5). The proportionality constant α_m was determined for each calendar month by means of a regression of the observed values of PET for the Belgian part of the basin on the observed daily temperatures. The values of α_m range from approximately 0.08 °C^{-1} in the summer half-year to 0.13 °C^{-1} in the winter half-year. These values are considerably lower than the value 0.17 °C^{-1} used by LBAW05.

Fig. 11 shows the mean annual cycle of the discharge as simulated by HBV with observed precipitation and temperature and with corrected and uncorrected data from the HadAM3H-driven run. Although the annual cycle of the mean discharge from the RACMO data appears realistic, the mean discharge during December–February is overestimated if no bias correction is applied. This is a result of the bias in the mean winter precipitation, shown in the left panel of Fig. 2.

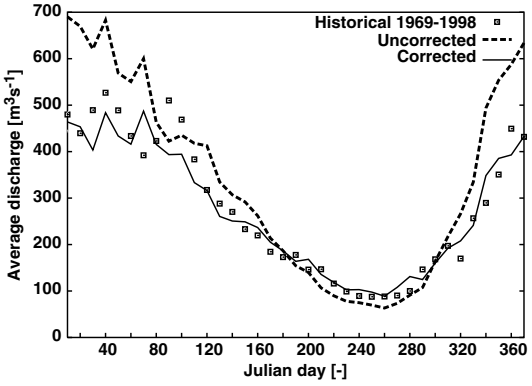

Figure 11 Mean annual cycle of the 10-day average discharge simulated by HBV with observed precipitation and temperature (historical, squares) and with corrected and uncorrected data from the HadAM3H-driven run.

Fig. 12 compares the Gumbel plots of the discharge winter maxima as obtained from the bias-corrected 30-year RACMO runs (using the nonlinear correction) with those simulated using observed data. There is a close correspondence between the plots for the HBV simulation with bias-corrected RACMO data and the plot for the HBV simulation with observed data, except for the two highest maxima from the HadAM3H-driven run. The two highest maxima in the simulation with observed data correspond with two known flood events in December 1993 and January 1995. In the ERA40-driven run these two events are reproduced correctly, because they are related to large-scale weather features, which influence RACMO through the boundary conditions.

Fig. 12 further shows the Gumbel plots of the discharge winter maxima resulting from the use of the resampled sequences from RACMO data. The plots are similar to those of the corresponding 10-day precipitation maxima in Fig. 10. There are marked differences between the plots for the

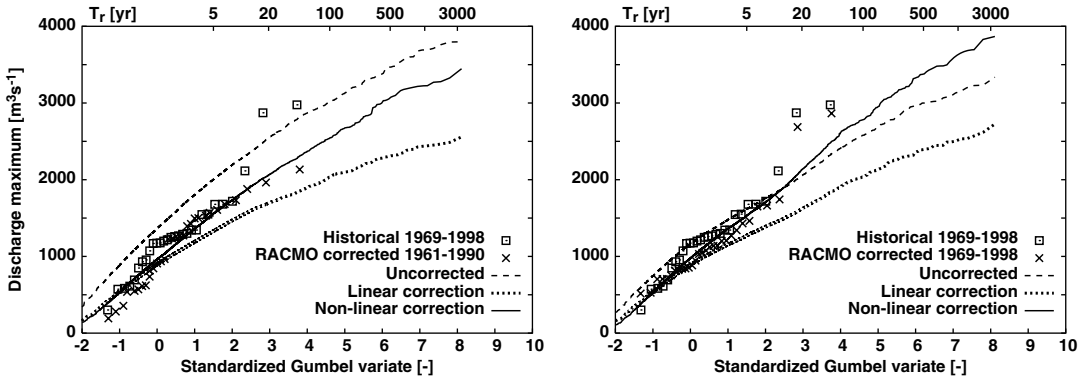

Figure 12 Winter maxima of discharge as simulated by HBV with observed meteorological data (squares), nonlinearly corrected RACMO data (crosses) and resampled RACMO data (9000 years), either uncorrected or with a linear or a nonlinear correction. The exponent b of the nonlinear correction was based on CV_1 for the HadAM3H-driven run in the left panel and on CV_{10} for the ERA40-driven run in the right panel.

HBV simulations with uncorrected resampled RACMO data and those for the simulations with observed precipitation and temperature. The differences are even larger if a linear correction is applied to the precipitation input data. The quantiles of the distribution of the winter discharge maxima are then underestimated considerably as a result of the underestimation of the CVs of the multi-day precipitation amounts. For the nonlinearly corrected precipitation input data, the resulting Gumbel plots are much closer to those obtained with observed precipitation and temperature. The correction of the variability of multi-day precipitation is thus essential for a realistic simulation of the discharge maxima. A matter of concern is that the simulated maxima for December 1993 and January 1995 are clearly above the plots for the resampled data for both the HadAM3H-driven run and the ERA40-driven run. This also occurs with resampling from the observed daily precipitation and temperature (LBAW05). The December 1993 and January 1995 maxima would have been plotted at a longer return period if longer discharge simulations were available. The 95-year discharge record at Borgharen contains only one other event (January 1926) that is comparable with the floods of December 1993 and January 1995.

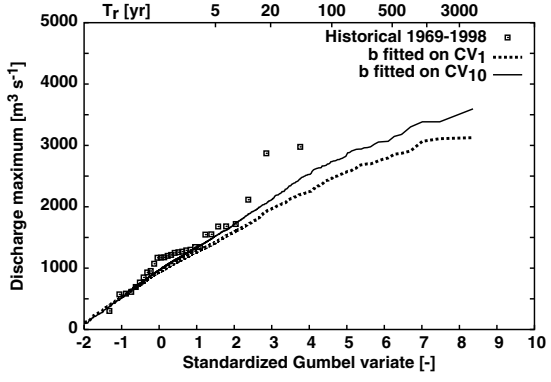

Figure 13 Discharge winter maxima from two 3000-year HBV simulations based on the resampled ERA40-driven RACMO run. Both simulations are based on the same resampled 3000-year sequences, but with different values of the correction parameter b, based respectively on CV_1 and CV_{10}.

For the ERA40-driven run, Fig. 13 shows the effect of using different CVs for fitting the exponent b in the nonlinear correction on the simulated winter discharge maxima. For return periods beyond five years the correction based on CV_1 results in rather low quantiles compared to those obtained with observed precipitation. A better agreement is achieved if b is fitted on CV_{10}. For the HadAM3H-driven run the differences are small (not shown). Nevertheless, for the Meuse basin it is recommendable to base the value of b on CV_{10} rather than CV_1.

Conclusion and summary

In this study output of the KNMI regional climate model RACMO was resampled with a nearest-neighbour technique to produce long-duration sequences of daily precipitation and temperature for the Belgian and French subbasins of the river Meuse. Bias corrections were applied to synthetic 3000-year sequences of precipitation and temperature to reproduce statistical properties of observed data. With the bias-corrected resampled sequences the daily discharge in Borgharen was simulated with the HBV rainfall—runoff model.

It was found that the correction for the bias in the mean precipitation by linear scaling of the daily precipitation amounts leads to an underestimation of large quantiles of their distribution. As a result, the occurrence of extreme river flows is underestimated considerably. This problem was encountered with both model runs in this study (either driven by HadAM3H or ERA40). A marked improvement was achieved with a nonlinear transformation, adjusting the mean as well as the CV of daily precipitation. For the ERA40-driven run even better results for extreme river flows were obtained by fitting the exponent in the nonlinear correction on the CV of the 10-day precipitation amounts. Despite a slight overestimation of the daily variability and a negative bias in the autocorrelation coefficients of the daily precipitation amounts, the distribution of the 10-day precipitation maxima is reproduced adequately. In order to reproduce the distribution of extreme discharges for a relatively large river basin like that of the Meuse, it is generally more appropriate to correct for biases in statistical

properties of the multi-day precipitation totals instead of daily precipitation.

The used correction does not adjust the frequency of wet days. Biases in the wet-day frequency, or more general, the left tail of the frequency distribution of daily precipitation have usually little influence on the distribution of extreme river flows. However, the CVs of both the daily and multi-day precipitation amounts depend on the wet-day frequency. As a result, the nonlinear transformation may do less well for RCM simulations having a larger bias in the wet-day frequency than the RACMO simulations considered in this study. The bias in the autocorrelation (and the spatial correlation) of the simulated daily precipitation amounts may also restrict the use of this transformation.

The flood quantiles simulated with the bias-corrected resampled RCM precipitation resemble those simulated with observed precipitation quite well. The next question is whether the presented approach can successfully be applied to the output of RCM scenario runs. This question will be addressed in a subsequent study.

Acknowledgements

The work was performed in co-operation with the Institute for Inland Water Management and Waste Water Treatment (RIZA) as the first stage of the development of a weather generator for the Meuse basin under changed climatic conditions. Special thanks are due to Marcel de Wit for conducting and analyzing the HBV simulations and for sharing his expertise in numerous fruitful discussions. The station records and subbasin data for the Belgian part of the Meuse basin were kindly provided by the Royal Meteorological Institute of Belgium. The French station data were made available by Météo France. The RACMO data were generously provided by Bart van den Hurk. Last but not least the authors thank two anonymous reviewers for their comments on an earlier version of the paper.

References

Arnell, N.W., Reynard, N.S., 1996. The effects of climate change due to global warming on river flows in Great Britain. Journal of Hydrology 183, 397–424.

Arnell, N.W., Hudson, D.A., Jones, R.G., 2003. Climate change scenarios from a regional climate model: estimating change in runoff in southern Africa. Journal of Geophysical Research 108 (D16), 4519. doi:10.1029/2002JD002782.

Booij, M.J., 2005. Impact of climate change on river flooding assessed with different spatial model resolutions. Journal of Hydrology 303, 176–198.

Buishand, T.A., Beersma, J.J., 1993. Jackknife tests for differences in autocorrelation between climate time series. Journal of Climate 6, 2490–2495.

Buishand, T.A., Brandsma, T., 2001. Multisite simulation of daily precipitation and temperature in the Rhine basin by nearest-neighbor resampling. Water Resources Research 37, 2761–2776.

Christensen, J.H., Christensen, O.B., in press. A summary of the PRUDENCE model projections of changes in the European climate by the end of this century. Climatic Change.

Frei, C., Christensen, J.H., Déqué, M., Jacob, D., Jones, R.G., Vidale, P.L., 2003. Daily precipitation statistics in regional climate models: evaluation and intercomparison for the European Alps. Journal of Geophysical Research 108 (D3), 4124. doi:10.1029/2002JD002287.

Hay, L.E., Clark, M.P., Wilby, R.L., Gutowski Jr., W.J., Leavesley, G.H., Pan, Z., Arrit, R.W., Takle, E.S., 2002. Use of regional climate model output for hydrologic simulations. Journal of Hydrometeorology 3, 571–590.

Jones, R., Murphy, J., Hassel, D., Taylor, R., 2001. Ensemble mean changes in the simulation of the European climate of 2071–2100 using the new Hadley Centre regional modelling system HadAM3H/HadRM3H. Hadley Centre Report, March 2001, p. 19.

Kay, A.L., Jones, R.G., Reynard, N.S., 2006. RCM rainfall for UK flood frequency estimation. II. Climate change results. Journal of Hydrology 318, 163–172.

Leander, R., Buishand, T.A., Aalders, P., de Wit, M.J.M., 2005. Estimation of extreme floods of the river Meuse using a stochastic weather generator and a rainfall–runoff model. Hydrological Sciences Journal 50, 1089–1103.

Lenderink, G., Buishand, T.A., van Deursen, W., in press. Estimates of future discharges of the river Rhine using two scenario methodologies: direct versus delta approach. Hydrology and Earth System Sciences.

Lenderink, G., van den Hurk, B.J.J.M., van Meijgaard, E., van Ulden, A.P., Cuijpers, H., 2003. Simulation of present-day climate in RACMO2: first results and model developments. Technical Report TR-252, Royal Netherlands Meteorological Institute, De Bilt.

Lindström, G., Johansson, B., Persson, M., Gardelin, M., Bergström, S., 1997. Development and test of the distributed HBV-96 hydrological model. Journal of Hydrology 201, 272–288.

Mearns, L.O., Hulme, M., Carter, T.R., Leemans, R., Lal, M., Whetton, P., 2001. Climate scenario development. In: Houghton, J.T. et al. (Eds.), Climate Change 2001: the Scientific Basis, Contribution of Working Group I to the Third Assessment Report of the Intergovernmental Panel on Climate Change. Cambridge University Press, Cambridge/New York, pp. 739–768.

Nijssen, B., O'Donnel, G.M., Hamlet, A.F., Lettenmaier, D.P., 2001. Hydrologic sensitivity of global rivers to climate change. Climatic Change 183, 397–424.

Prudhomme, C., Reynard, N., Crooks, S., 2002. Downscaling of global climate models for flood frequency analysis: where are we now? Hydrological Processes 16, 1137–1150.

Rajagopalan, B., Lall, U., 1999. A *k*-nearest-neighbor simulator for daily precipitation and other variables. Water Resources Research 35, 3089–3101.

Shabalova, M.V., van Deursen, W.P.A., Buishand, T.A., 2003. Assessing future discharge of the river Rhine using regional climate model integrations and a hydrological model. Climate Research 23, 233–246.

Tu, M., 2006. Assessment of the effects of climate variability and land use change on the hydrology of the Meuse river basin. PhD thesis, UNESCO-IHE, Delft, the Netherlands.

Uppala, S.M. et al., 2005. The ERA-40 re-analysis. Quarterly Journal of the Royal Meteorological Society 131, 2961–3012.

van Ulden, A., Lenderink, G., van den Hurk, B., van Meijgaard, E., in press. Circulation statistics and climate change in central Europe: PRUDENCE simulations and observations. Climatic Change.